MICROMACHINED STIMULATING ELECTRODES

Quarterly Report #11

(Contract NIH-NINDS-N01-NS-5-2335)

April - June 1998

Submitted to the

Neural Prosthesis Program
National Institute of Neurological Disorders and Stroke
National Institutes of Health

by the

Center for Integrated Sensors and Circuits
Department of Electrical Engineering and Computer Science
University of Michigan
Ann Arbor, Michigan
48109-2122

July 1998

THIS QPR IS BEING SENT TO YOU BEFORE IT HAS BEEN REVIEWED BY THE STAFF OF THE NEURAL PROSTHESIS PROGRAM.

MICROMACHINED STIMULATING ELECTRODES

Summary

This program seeks to develop a family of thin-film stimulaing arrays for use in neural prostheses. During the past quarter, work has gone forward in a number of areas. We have continued to explore alternative processing options for defining the silicon substrate which shapes these probes, especially the use of a porous silicon sacrificial layer. Such layers can be undercut from the front so that the probes do not have to be released by etching completely through the wafer. Furthermore, they can be released at room temperature such that the etchants involved do not attack any of the other materials used. Previously, a boron-doped buried layer was used for the porous sacrificial layer; however, during the past term, we have found that an n+ buried layer works better, outdiffuses less, and can be released using a single electrochemical electropolishing etch at end of process so that no actual porous silicon is involved. We are using this technique on a set of probes that are currently in fabrication. This set includes a 32-site 46mm-long stimulating probe for use in the cochlea. This study will be completed during the coming term and contrasted with the usual boron-diffused etch-stop process.

During the past term, the active probes STIM-2B and -3B have been completed. STIM-2B is a 64-site 4-channel 16-shank probe that routes each of the input channels to one of 16 sites under the control of a serial input data stream. These probes have been tested and found fully functional. The yield of the probes was high, reflecting the improved methods for protecting the active circuit areas mentioned in the past report. The maximum data input rate on the probes in our present test setup is 4MHz, very close to the design value. The current pattern launched by the probe can thus be altered in about 4μsec. All of the operating modes of the probes are functional, including power-on reset (POR) for site activation and the high-impedance test mode for testing leakage on the overall structure. Any of the selected sites can be used for recording or stimulation. The on-chip recording amplifiers have a maximum gain at 1KHz of at least 40dB and a low-frequency rolloff below 100Hz. These devices have been used with the external electronic interface developed for the stimulating probes and have been found to operate well. Undercut gold fuses have also been demonstrated for use in coding future 3D platforms to allow different numbers of the STIM-3B probes to be used as desired. The STIM-3B probes are also fully functional and are built around STIM-2B with the addition of an on-chip x-address register and wings for mounting in the 3D assembly.

During the coming term, we will complete the study of alternative substrate definition techniques and will test the STIM-2B probes in-vivo. In addition, several 3D arrays of STIM-3B probes will be assembled. We will then move to a final iteration of our 64-site 8-channel 16-shank probe with on-chip current generation, STIM-2, and its 3D counterpart, STIM-3.

MICROMACHINED STIMULATING ELECTRODES

1. Introduction

The goal of this research is the development of active multichannel arrays of stimulating electrodes suitable for studies of neural information processing at the cellular level and for a variety of closed-loop neural prostheses. The probes should be able to enter neural tissue with minimal disturbance to the neural networks there and deliver highly-controlled (spatially and temporally) charge waveforms to the tissue on a chronic basis. The probes consist of several thin-film conductors supported on a micromachined silicon substrate and insulated from it and from the surrounding electrolyte by silicon dioxide and silicon nitride dielectric films.. The stimulating sites are activated iridium, defined photolithographically using a lift-off process. Passive probes having a variety of site sizes and shank configurations have been fabricated successfully and distributed to a number of research organizations nationally for evaluation in many different research preparations. For chronic use, the biggest problem associated with these passive probes concerns their leads, which must interface the probe to the outside world. Even using silicon-substrate ribbon cables, the number of allowable interconnects is necessarily limited, and yet a great many stimulating sites are ultimately desirable in order to achieve high spatial localization of the stimulus currents.

The integration of signal processing electronics on the rear of the probe substrate (creating an "active" probe) allows the use of serial digital input data which can be demultiplexed on the probe to provide access to a large number of stimulating sites. Our goal in this area is to develop a family of active probes capable of chronic implantation in tissue. For such probes, the digital input data must be translated on the probe into per-channel current amplitudes which are then applied to the tissue through the sites. Such probes generally require five external leads, virtually independent of the number of sites used. As discussed in previous reports, we have designed a series of active probes containing CMOS signal processing electronics. Two of these probes have been completed and are designated as STIM-1A and STIM-1B. A third probe, STIM-2, is now undergoing a final iteration and is a second-generation version of our original high-end first-generation design, STIM-1. All three probes provide 8-bit resolution in digitally setting the per-channel current amplitudes. STIM-1A and -1B offer a biphasic range using ±5V supplies from 0μA to ±254μA with a resolution of 2μA, while STIM-2 has a range from 0 to ±127μA with a resolution of 1μA. STLM-2 offers the ability to select 8 of 64 electrode sites and to drive these sites independently and in parallel, while STIM-1A allows only 2 of 16 sites to be active at a time (bipolar operation). STIM-IB is a monopolar probe, which allows the user to guide an externally-provided current to any one of 16 sites as selected by the digital input address. The high-end STLM-2 contains provisions for numerous safety checks and for features such as remote impedance testing in addition to its normal operating modes. It also offers the option of being able to record from any one of the selected sites in addition to stimulation. It will be the backbone of a multi-probe three-dimensional (3D) 1024-site array (STIM-3) now in development. A new probe, STIM-2B, has now been added to this set. It offers 64-site capability with off-chip generation of the stimulus currents for four separate channels. These channels are organized in four groups so that each current can be directed to any of the 16 sites in its group, and the site can be programmed for either stimulation or recording. This probe is available in both 2D and 3D versions (as STIM-2B/3B).

During the past quarter, we have continued to fabricate passive probe structures for internal and external users. We have also continued to explore the use of a porous silicon sacrificial layer for probe release as a possible alternative to the boron-diffusion process now used. This study will be completed during the coming term. The STIM-2B/3B probes were successfully completed and have now been tested. They are fully functional and have been used with the external interface hardware developed for this purpose. A printed-circuit-board version of this hardware is now in development to aid in the use of these probes by both internal and external users. The results in each of these areas are described more fully in the sections below.

2. Development of a Surface Micromachining Technology for Active Probe Fabrication

As outlined in previous quarterly reports, we have been exploring several process alternatives for use in defining the probe substrate to see whether they might offer significant advantages over the boron-diffusions that have become traditional in this role. The principal approach being explored uses a porous silicon layer, formed by electrochemically etching a buried sacrificial silicon layer, to allow release of the probe structure without etching through the entire wafer. This release can be performed at room temperature, where the silicon etch does not significantly attack even exposed aluminum. Avoiding the long through-wafer etch is increasingly attractive as wafer sizes, and thicknesses, increase. The porous process might also be more easily adapted to foundry fabrication as the probes move outside the university to commercial use.

A run of wafers is now in progress using the porous silicon process technology. As discussed previously, this technique uses an electrochemical etch in hydrofluoric acid (HF) to create a sacrificial layer in the bulk silicon. The probes are first defined by dry etching their shapes and thicknesses into the substrate and then growing epitaxial silicon (epi) to fill these trenches and form the device material. At the end of the process, rather than etching through the entire thickness of the wafer, the sacrificial layer is removed to lift out the probes. Unlike standard surface micromachining processes, this technique allows the surface micromachined structures to be monocrystalline silicon and several tens of microns thick if desired.

Process development has continued this quarter and several changes have been made to the wafer doping profile and the way in which the micromachining steps are integrated with a standard CMOS process. It was previously thought that processing would take place on a p-type wafer and that a p+ buried layer beneath the epi would be used for the sacrificial material. A thin bottom layer of n-type epi, followed by a 15μm-thick layer of lightly-doped p-type epi would be grown to form the device silicon. Circuitry would be fabricated in the p-type layer using an n-well CMOS process, while the n-type layer would form an outer grounded surface on the completed probes. The p+ layer would be made porous midway through the process by electrochemical etching in HF, then removed in room-temperature KOH at the end of the process to lift out the probes. Several problems were discovered, however, with using a p+ sacrificial layer. First, when a p+ layer is made porous, the rate of pore formation in the lateral direction is too slow to undercut structures wider than several hundred microns in a reasonable amount of time and without forming pores through the entire thickness of the wafer. Secondly, the p+ dopant (boron) diffuses very rapidly at high temperatures, causing the p+ buried layer to widen during furnace steps prior to being made porous, thereby greatly reducing the thickness of the probes themselves.

It was determined that the doping profile of the wafer needed to change in order to eliminate these problems. In experimenting with different profiles, it was found that when n+ silicon is used for the sacrificial layer, the results of the electrochemical etch are quite different. Rather than the layer beneath the epi being made porous, it is electropolished, or completely removed. Although this eliminates the ability to perform further processing after the electrochemical etch, it provides a way to form and remove the sacrificial layer in a single, final step. In addition to eliminating the KOH etch step, this approach makes the process more CMOS compatible by placing all micromachining steps at the end of the process. Additionally, the rate of lateral undercutting is much greater with electropolishing than with porous silicon formation, making it possible to undercut and lift out 2mm-wide structures in approximately 10 minutes. When the buried layer is electropolished, however, the silicon above and below it slowly becomes porous. A pn-junction placed within the epi forms an etch-stop to this pore formation. A double epi layer is again used, with a thin p-type bottom layer and a 15μm-thick n-type top layer. When the n+ layer is electropolished, pores form in the p-type silicon but stop at the edge of the n-type layer. Circuitry is fabricated in the lightly-doped n-type silicon using a standard p-well CMOS process.

There are several questions which need to be answered regarding the effects of this new process on the performance of the probes. It is possible that the use of a lightly-doped substrate for the shanks will cause an increase in noise due to an increase in light generation. There may also be changes in the mechanical properties of the substrate due to internal stress changes in the absence of a high concentration of incorporated boron. These questions and others will be answered when implants are performed with the completed probes.

A mask set which includes 32-site active cochlear implant stimulating probes and 5-site passive recording probes was completed during this quarter. Fabrication using this mask set and the new micromachining process is currently in progress. The cochlear implant is designed to stimulate four channels simultaneously. Site selection is performed on-board, while the currents are generated externally. A series of eight polysilicon strain gauges was placed on the front-end insertable portion of the implant and will be used to measure bending of the substrate during and after insertion into the spiral cochlea. One of the eight gauges is selected at a time (on-chip) and its output compared with that of a back-end reference resistor in order to reduce temperature effects. Readings from the eight gauges can be put together to form a piecewise image of the implanted substrate, which should be a valuable tool to surgeons for inserting and monitoring the position of such implants.

While this porous/electropolishing process is not intended to replace the boron etch-stop bulk-micromachining process, it does offer potential advantages for several applications. Unlike the current process, it provides an etch-stop on all sides of circuit areas and, as a result, totally eliminates etch timing in release of the probes from the host wafer. It would also allow some circuitry to be moved from the back end of the probe to the shanks, decreasing the back end profile and enabling the number of sites to be increased without the number of leads increasing proportionally. This is especially important for 4.6cm-long cochlear implant probes, where wide leads are desirable to reduce voltage drops along the current lines. The primary disadvantage of the new process appears to be its increased cost and complexity over the current process. It does, however, use processes that are foundry standard (epi growth, CMP) and compatible (electropolishing in HF) for the micromachining steps. All of the advantages and disadvantages of this new process technology and its potential use in fabricating neural probes will be evaluated as this processing study is concluded during the coming quarter.

3. *Active Stimulating Probe Development*

During the past quarter, work on active stimulating probes has focused on the completion of the active stimulation probe set, STIM-2B/3B. As reported last quarter, this mask set was carried through the CMOS portion of the fabrication, and the test results at that point looked very encouraging; the device parameters were close to expected values and circuit blocks were functioning as expected. We have now completed the post-CMOS processing, which includes passivation, site and pad formation, wafer thinning, and the final probe release etch. We have tested the probes both with a test bench setup and with our external interface system; in both cases the probes performed very well -- almost better than expected. Testing of the etched-out probes has demonstrated that the digital logic is functional and the analog amplifier works as designed. The final etch-out has often been problematic in the past due to the difficulties in protecting the circuitry from attack by the EDP (ethylene diamine pyrocatechol) etchant. The good etch-out results here have validated our new method of protecting the circuit areas from undercutting using dielectric bridges at the corners of these areas. We have also tested a method using microfuses to make the 3D array platforms programmable, and the results look very promising. These platforms will be used to realize 3D arrays of the STIM-2B probe designs.

STIM-2B

STIM-2B is a second-generation probe, a version of our simplest active stimulating probe, STIM-1B. STIM-2B is a four-channel, 16-shank, 64-site probe which routes each of four externally-generated stimulus signals to 1-of-16 sites. The fabrication of the CMOS circuitry has been completed, and the digital functionality of the circuitry has been verified by testing of the different modes of the probe: POR, site selection, amplifier selection, and so forth. Testing of the analog amplifier has demonstrated that it too works quite well.

The functionality of the STIM-2B should provide an important tool for performing some very important and interesting experiments by allowing acute and chronic stimulation access to a relatively large volume of neural tissue without mechanically repositioning the probe. This capability is realized by utilizing a 20b shift register to load four 4b site addresses which are decoded by a 1-of-16 nand-type decoder to connect the desired site to an analog input/output pad through a large CMOS pass-gate transistor, thereby allowing the 'steering' of externally generated currents to the addressed site. A new recording function has been added and is addressed by a fifth bit included with the 4b site address. This fifth bit selects between stimulation mode and recording mode by selecting either a direct path to the I/O pad from the site or a path through an amplifier for recording from the same site. Each I/O channel has its own dedicated amplifier so that the functionality of all of the channels are independent of each other except for the up-front data input circuitry. A photograph of the completed etched-out STIM-2B probe circuitry is shown below in Fig. 1. Figure 2 is a SEM photograph which shows a closer view of a portion of the circuitry of the STIM-2B probe. Figure 3 is a SEM photograph of the backside of a STIM-2B probe which shows the effectiveness of the dielectric bridge corner protection method even though the probes were etched 15 minutes beyond the point of release and separation. A SEM photograph of an 80μm wide shank of the STIM-2B probe is shown in Fig. 4.

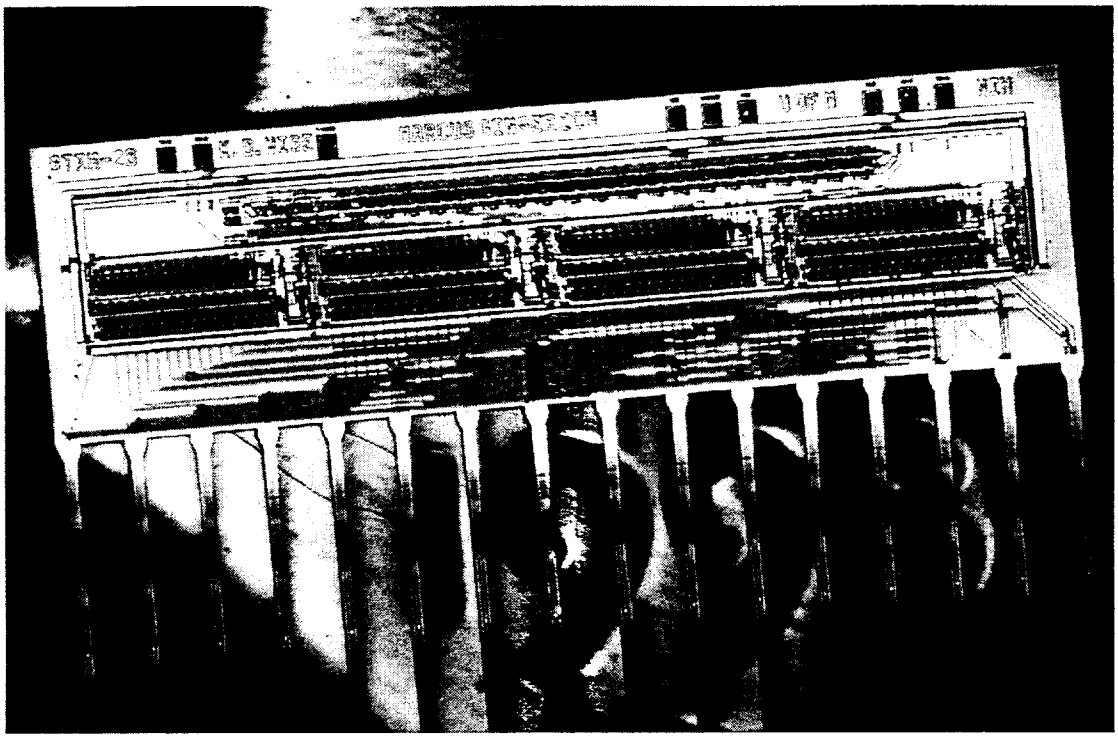

Fig. 1: A photograph of an etched-out STIM-2B probe. The shanks are on 400μm centers with four sites per shank.

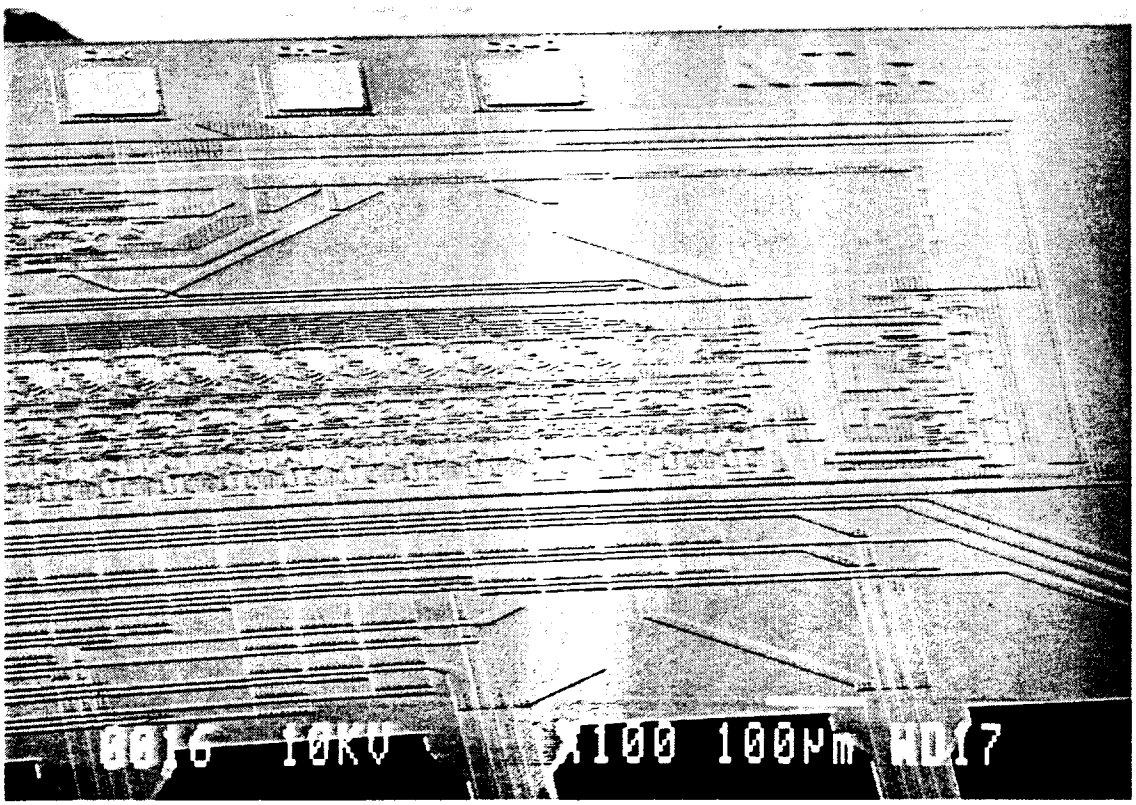

Fig. 2: A SEM photograph of the etched-out STIM-2B probe.

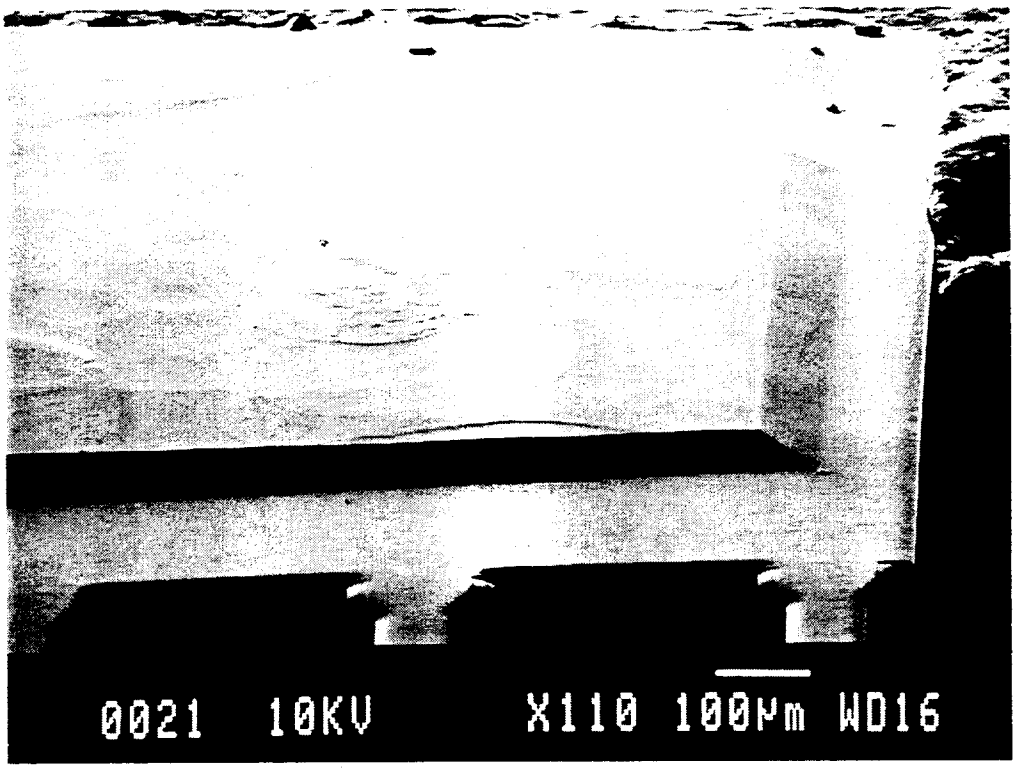

Fig. 3: A SEM photograph showing the backside of the etched-out STIM-2B probe. Even with a 15 minute over-etch, the circuitry is still well protected from attack by the etchant.

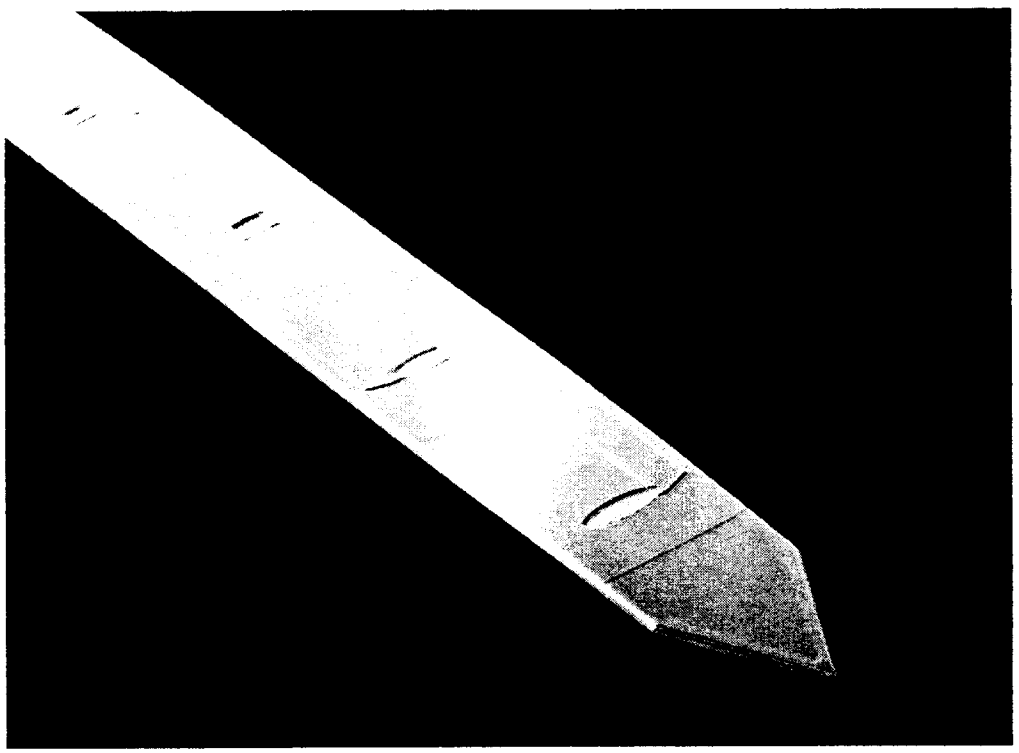

Fig. 4: A SEM photograph (X230) showing one of the sixteen 80µm wide, 4-site, shanks of the completed STIM-2B probe.

STIM-3B

STIM-3B is a three-dimensional probe that is an extension of the 2D probe, STIM-2B, and is setup to allow use in chronic experiments. There are no significant differences in these two probe designs, only some structural modifications to allow interconnection to a 3D platform assembly and a few minor circuit enhancements to allow the addressing of multiple probes in a 3D array.

The structural changes that were required, some of which can be seen in the photograph of the etched-out STIM-3B probe of Fig. 5, include the addition of 'wings' for 3D stabilization and "out-riggers " with integrated beam-lead interconnects for assembly and lead transfer from each probe to the 3D platform assembly. Also seen in the photograph, and in the SEM photograph of Fig. 7, are the 45° slots on the wings, which were designed such that a continuous trench would be etched from the front side of the probe even before the etch plane advances from the backside during the final release etch in EDP. A section of the STIM-3B probe shown in the SEM photograph of Fig. 6 shows a portion of the shift registers and the site-selector and amplifier of a single channel. A close-up of the electroplated gold beam-lead 90° transfer interconnects are shown in Fig. 8. Each interconnect is actually two beams lead for redundancy. Each half of the double beam is 40μm wide, with a 10μm separation between the two halves.

As discussed in previous reports, the integrity of the circuit area was ensured by making the surrounding deep boron diffused rim wide enough so that the lateral undercut from the corners does not have time to reach the active circuit area. The newly developed corner protection technique of using dielectric bridges and the anisotropy of the EDP etchant was also used to help improve the yield. Previous etch-out tests demonstrated the effectiveness of this technique, and the results of this fabrication run and subsequent etch-out have validated the technique on fully functional probes.

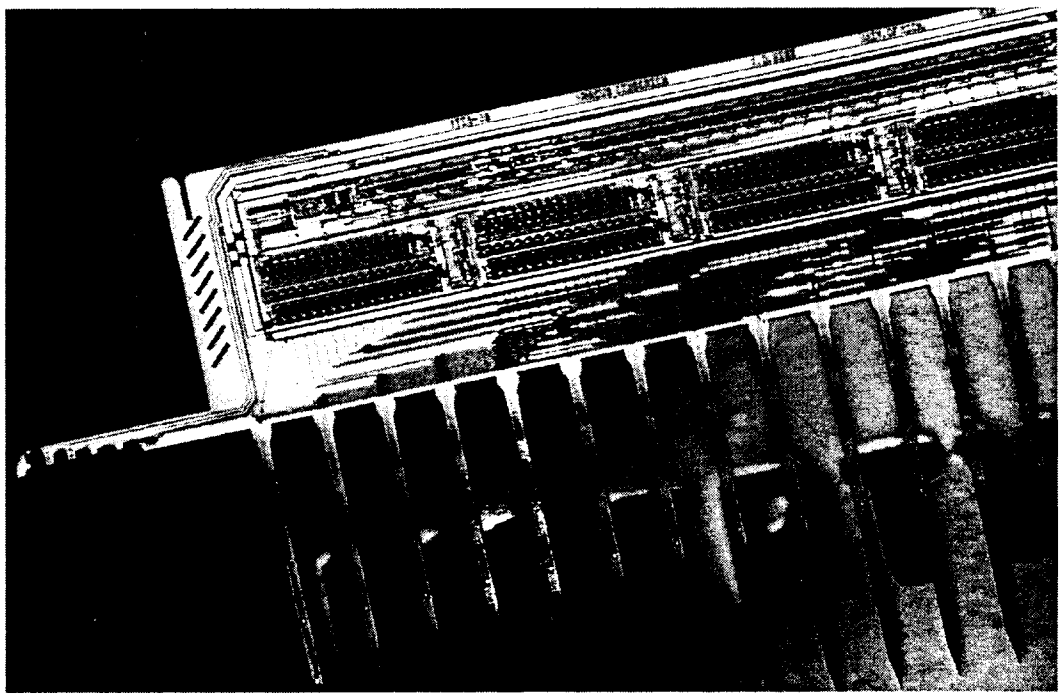

Fig. 5: Photograph of a completed STIM-3B probe. The shanks are on 400μm centers with 4 sites per shank.

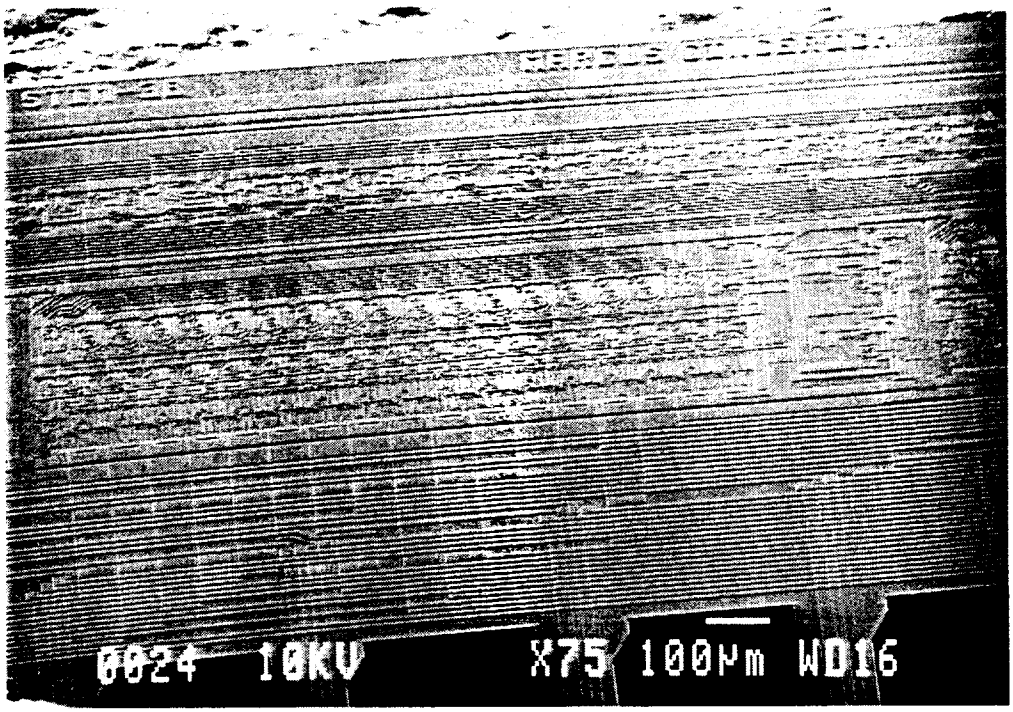

Fig. 6: An SEM photograph of an etched-out STIM-3B probe. Portions of the shift registers and strobe logic can be seen in the upper portion, while a single channel site selector and its associated amplifier can be seen at the middle left and right, respectively.

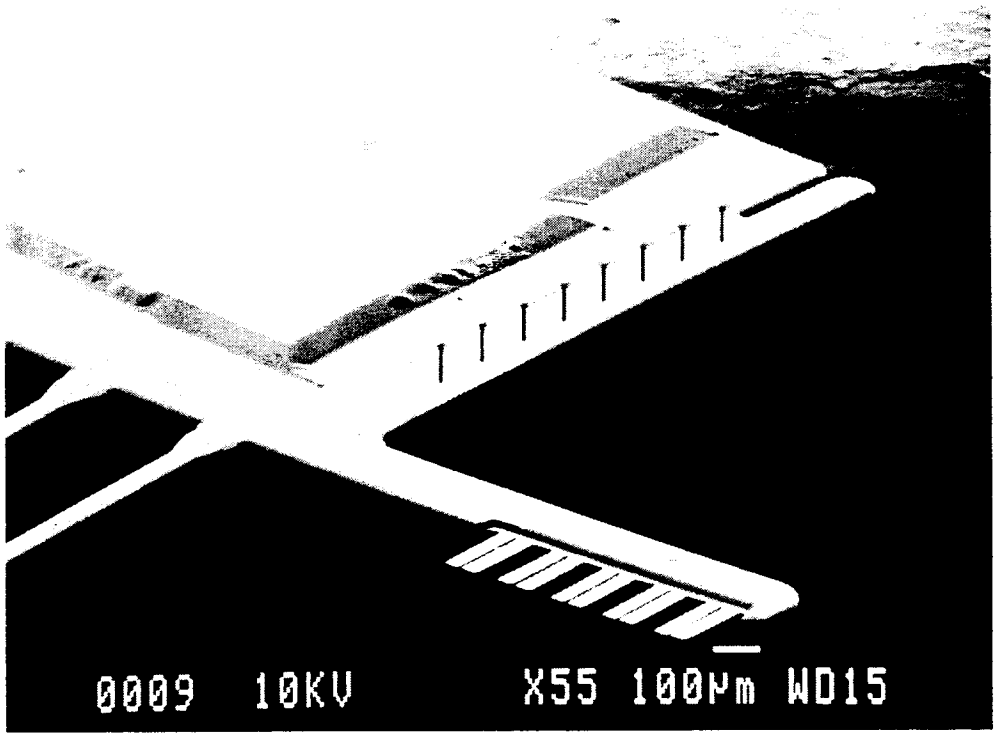

Fig. 7: A SEM photograph showing the backside of STIM-3B. The backside of the circuitry still remains protected even with a 15 minute over-etch beyond probe separation.

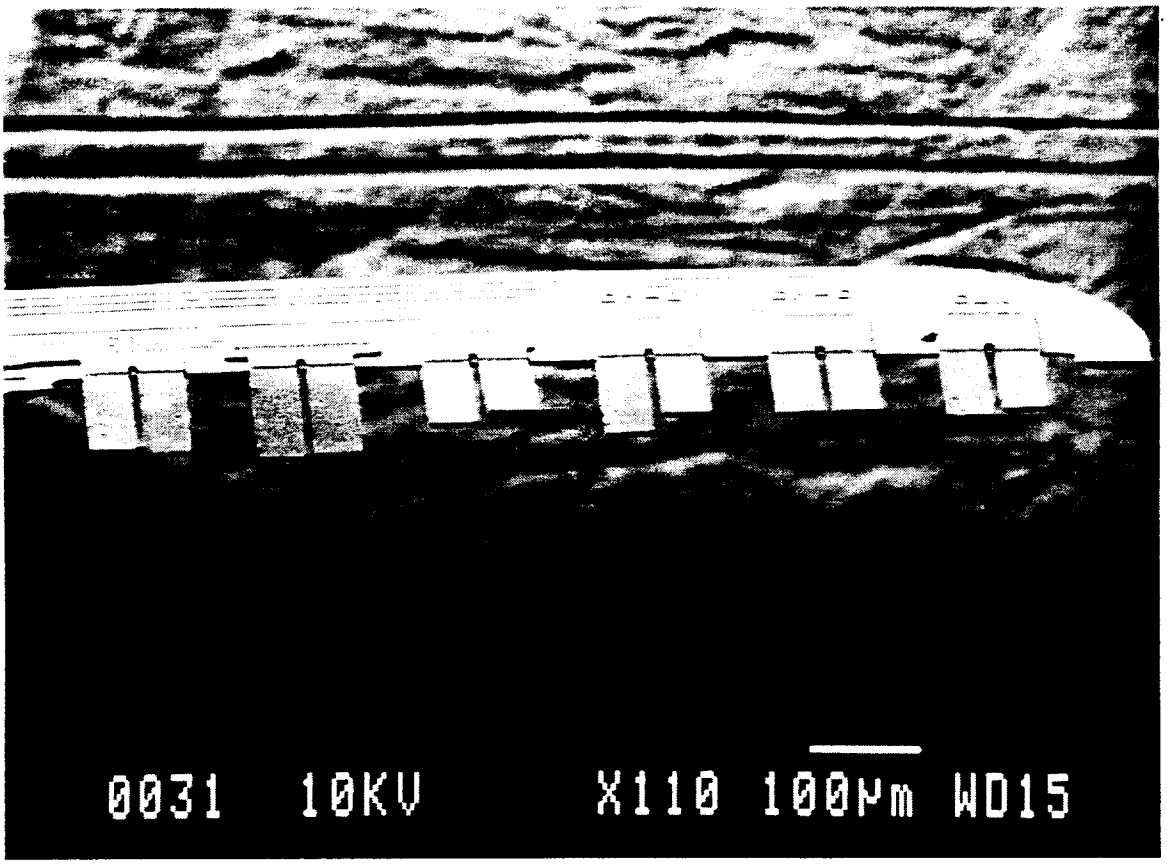

Fig. 8: A SEM photograph showing a close-up of some of the electroplated gold beam-lead 90° transfers of a completed STIM-3B probe. There are two lead tabs on each interconnect for redundancy. There is 60µm between interconnects; each beam is 40µm wide with a 10µm separation.

The minimal circuit changes necessary for the realization of STIM-3B included adding a 4b shift register, which flags the selection of an I/O line via a large CMOS passgate in the line. The last bit of the shift register is then buffered back out. This allows all the probes of a 3D system to share common analog I/O data lines, power lines, clock lines and y-addr (normal probe address) lines. The same y-addr is clocked into all the probes. Simultaneously, an x-addr (channel I/O enable) is clocked into the first probe and then daisy-chained to each successive probe in the array, making an extended 'virtual register.' This allows for different array sizes with only changes in the addressing from the outside driving circuitry. This creates a very flexible system with variable array sizes, inter-probe stimulations, and almost any combination of four sites across the array. The only weakness in this scheme is that the same I/O channel cannot be driven on more than one probe simultaneously with an independent stimulus current.

The STIM-2B/3B probes were designed to be very robust in that they should function even if the device target parameters are not met exactly. The only portion of the probe that is device-parameter sensitive is the amplifier used in the recording mode. The design was intended to be such that the probes will still function normally in the stimulation mode even if the amplifiers should not work due to device parameter shifts. The amplifiers have been tested, however, and shown to work as designed.

Circuit Test Results

Testing the functionality of the probe was done using a bench test setup which allowed us to look at the input and output waveforms at the same time on an oscilloscope. Using a standard integrated circuit testing probe and micromanipulator, the output from the different stimulation sites was observed by driving a 100μA current into the various channels of the probe and then observing the voltage drop across a 1kΩ resistor (see Fig. 9). An important result of the testing done on this probe was the determination that all of the digital and analog functions were working as expected.

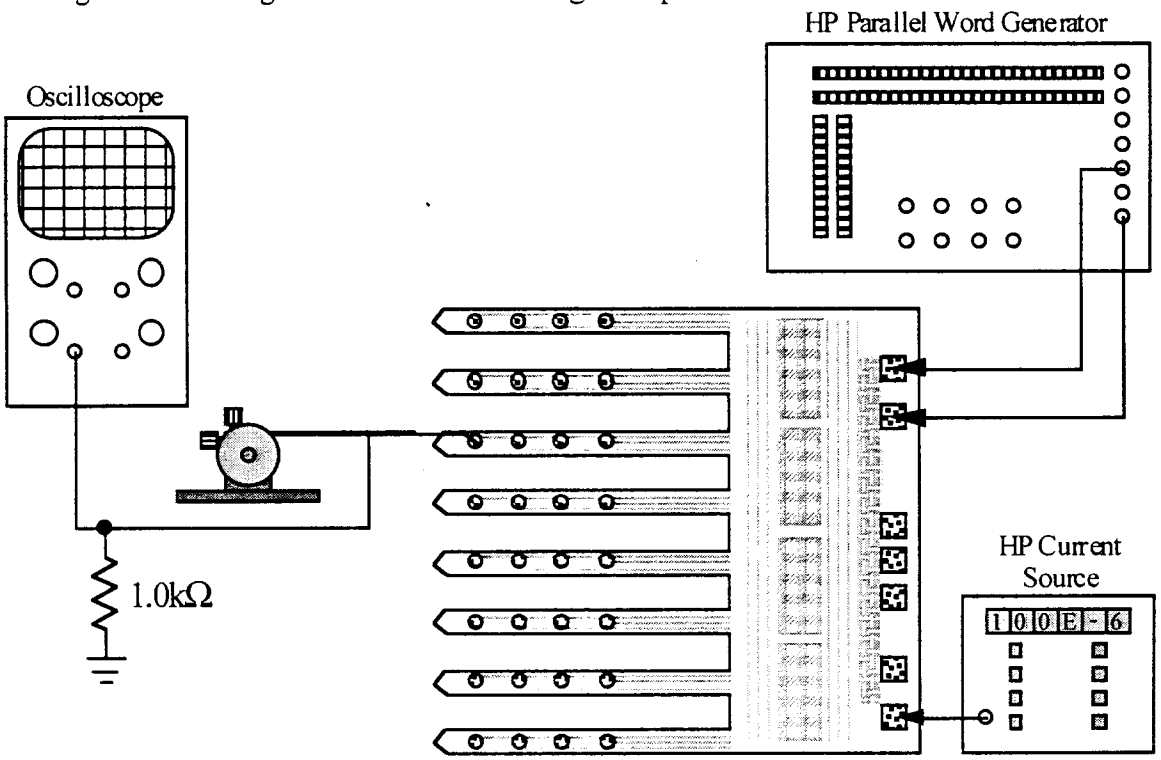

Fig. 9: A diagram of the test setup for conducting the functionality tests.

The functionality of the probe digital logic was demonstrated on the wafer in the previous quarterly report, but several sample photographs of oscilloscope traces from the completed probes are shown below in Figs. 10-13. These are a series of scope traces resulting from probing different sites while entering the same input to the probe. In each case, the top trace is the clock signal, the middle trace is the data input, and the bottom trace is the measured voltage across a 1kΩ resistor when probing the indicated site. Figure 10 is the result of probing site A0 (indicating site 0 of channel A). The signals are as expected. The strobe on the clock line resets the shift register to all zeros and selects ALL of the sites in parallel (for activation), the POR state; the next clock pulse turns off the POR state and site A0 is selected as expected. It can be seen that the subsequent single bit turns site A0 off as it clocks through the first 4b of the shift register (in which case a site other than A0 is selected) and then turns back on as the single one moves on thus leaving all zero's in the channel A site address. The strobe on the data line also resets the shift register to all zero's, but it does not select all of the sites in parallel; instead, while the strobe is held low A0 is turned off even though the shift register is set to all zero's. This mode is the high impedance mode and in this state, all sites are turned off so that a leakage current test can be performed.

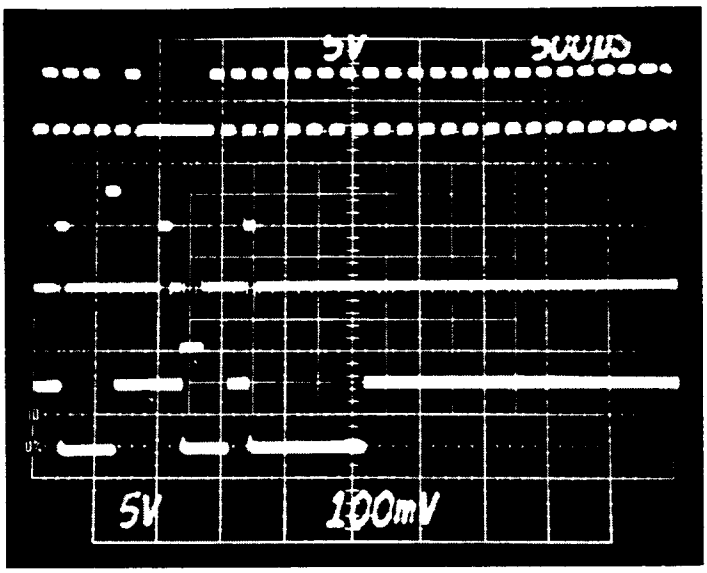

Fig. 10: A scope trace showing (top to bottom): clock, data, and output of site A0. The functionality of the POR state, POR reset, and leakage current mode are demonstrated.

The next example, Fig. 11, demonstrates the same input sequence as that used in Fig. 10, but site B2 is being monitored in the lower trace. Note the current source was changed to drive on channel B. Here we see again that the POR reset strobe on the clock line does have the effect of turning this channel just as is expected. We cannot see the effect of the data strobe because the channel is already off, but we can see that the channel turns on again after the reset and the single one is clocked through the shift register. Figure 12 shows the same input and resulting signal at site B3 which is the same as B1 except that the site is never selected as the single one is clocked through the shift register, which is exactly what it should do. The last example, Fig. 13, is of site D8 which is demonstrated because it shows that the single one completely traverses the length of the shift register to turn on the final bit of the channel D site address.

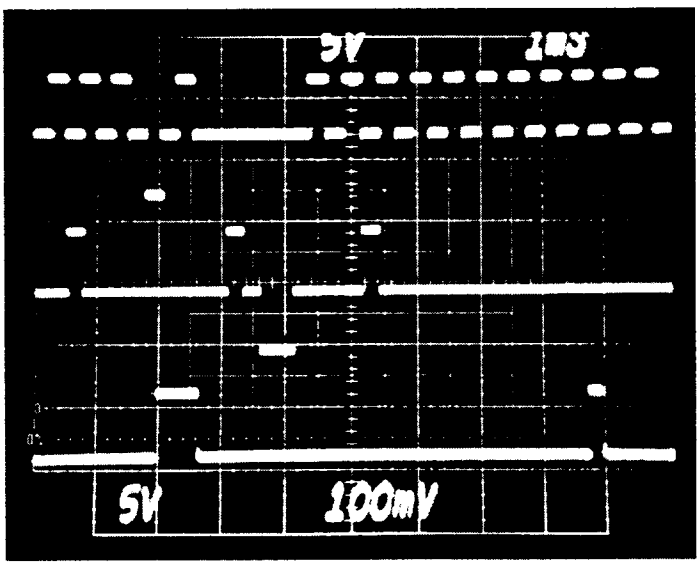

Fig. 11: Oscilloscope trace showing (top to bottom): clock, data, and output of site B2.

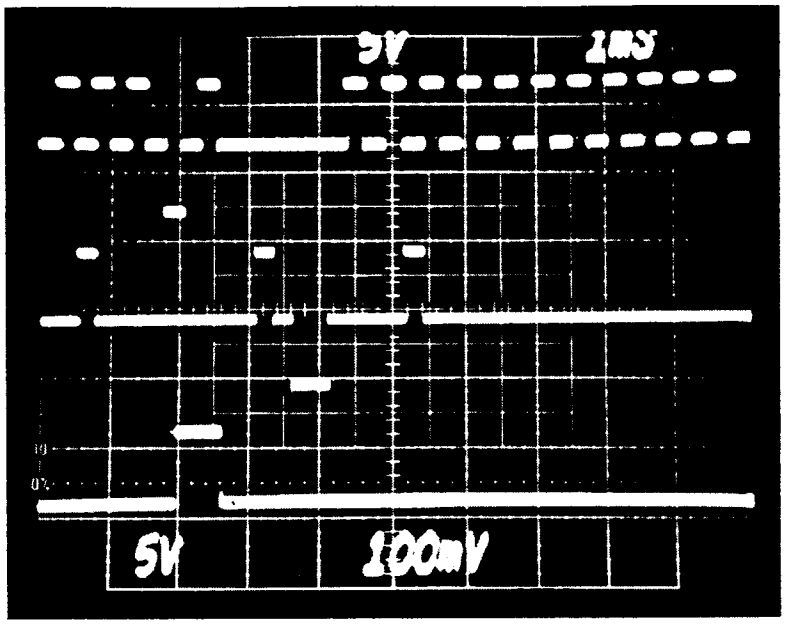

Fig 12: Oscilloscope trace showing (top to bottom): clock, data, and output of site B3.

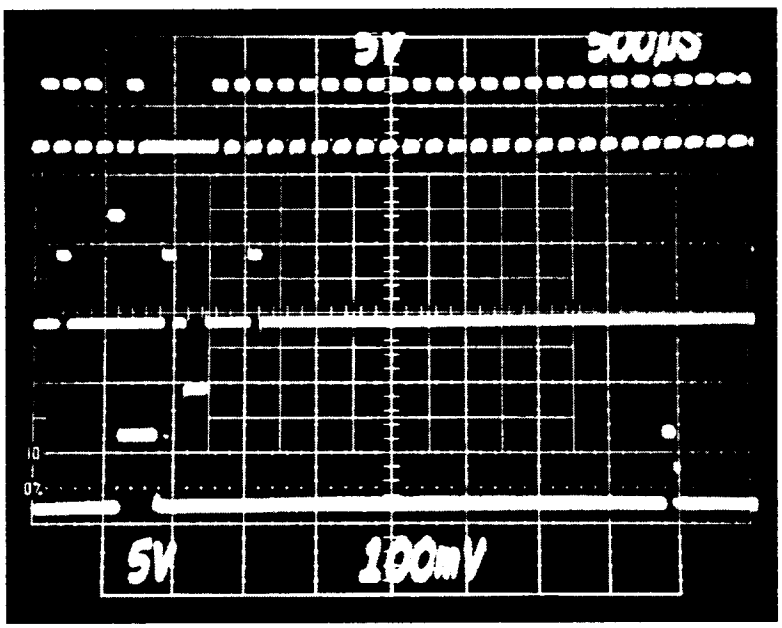

Fig. 13: Oscilloscope trace showing (top to bottom): clock, data, and output of site D8. This demonstrates the complete functionality of the shift register.

The main analog portion of these probes is the amplifier. This portion of circuitry is most sensitive to shifts in device parameters. If the amplifier circuits work, then these probes can be considered completely functional. As mentioned before, even if the amplifiers did not work, the probe should be able to be used for recording without any on-chip amplification. In order to look at the attenuation of the direct (stimulation) path, the frequency response, Fig. 14, was measured by turning the desired site on and connecting the appropriate channel. The response shows that the signal does not begin the degrade

until it reaches frequencies in the hundreds of kHz, well above the region of interest. The plot does seem to indicate a slight gain, but this is probably a calibration error in the measuring instrument.

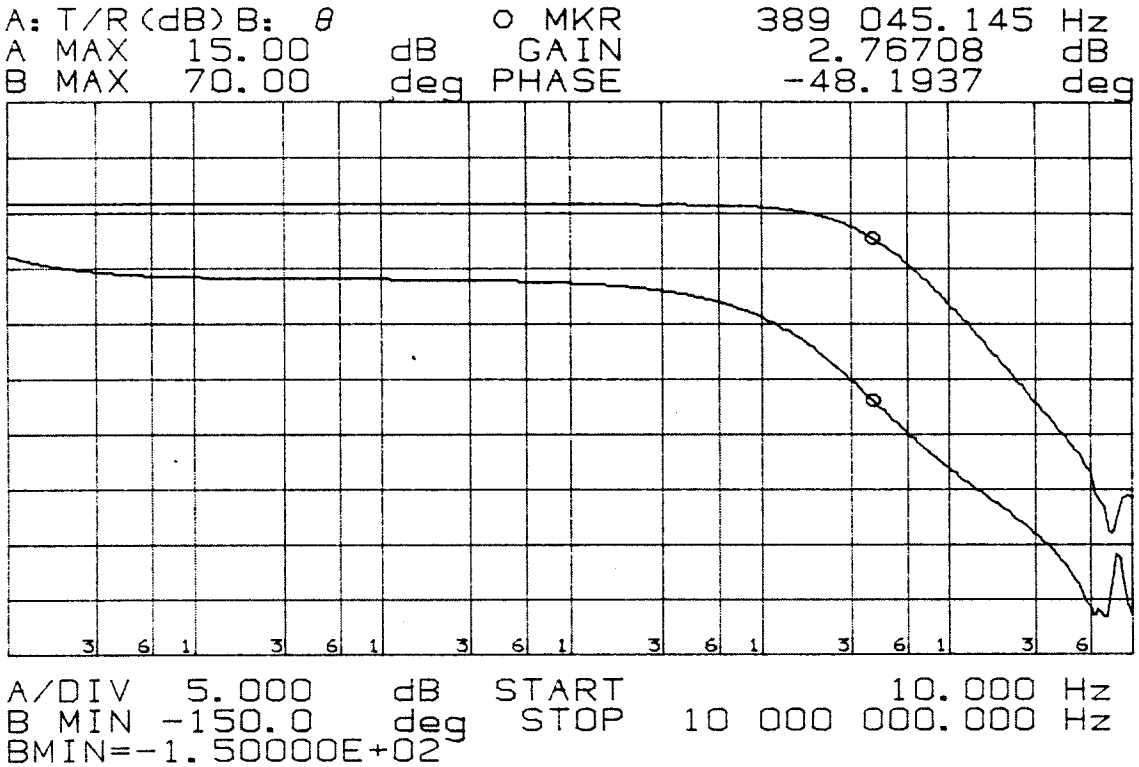

Fig. 14: The measured frequency response of a straight through (stimulation) path. Note, the slight offset from unity is probably due to measurement instrument miscalibration.

The frequency response of the amplifier on a completed probe was also tested by clocking in the necessary data to turn on the amplifier and select the probed site. Then, the frequency response was measured. The resulting measurement is shown below in Fig. 15. This measurement shows good low frequency attenuation which is desirable to eliminate low frequency voltage drift associated with the site metal/tissue interface. The response does have a high frequency roll-off that is a little lower than desired, probably as a result of the large capacitive load on the amplifier output as present in the test setup.

The probes were tested for their maximum data entry rate, and it was found that the clock and data could be entered at speeds of up to 4MHz. The probes were also tested in conjunction with the external interface system that has been developed and the complete system was found to work quite well.

Platform Development

In a previous quarterly report, we discussed a proposed technique for making the 3D platforms programmable in the number of probes which can be used in the array and where. This technique is a series of suspended gold beams (fuses) between the y-address data pads for the STLM-3B probes. The beams are formed during electroplating of the beam leads/pads and are then suspended by etching out an exposed (sacrificial) layer of

polysilicon during the final release etch. The suspension of the beam is desired to help provide thermal isolation, thus making it easier to 'blow' the fuse. A SEM photograph of such a beam is shown in Fig. 16. The array is programmed by 'blowing' the fuse wherever a possible probe position will be filled so that the probe is included in the extended 'virtual register'. It was not completely clear that the method would actually work, so several test structures were included on the recently completed mask set for evaluation. Figure 17 shows a fuse which was blown by applying 2V across it. The success of the initial tests would indicate that this may indeed be viable method for making the array platforms programmable, thus making it possible to have a standard platform for many different size arrays.

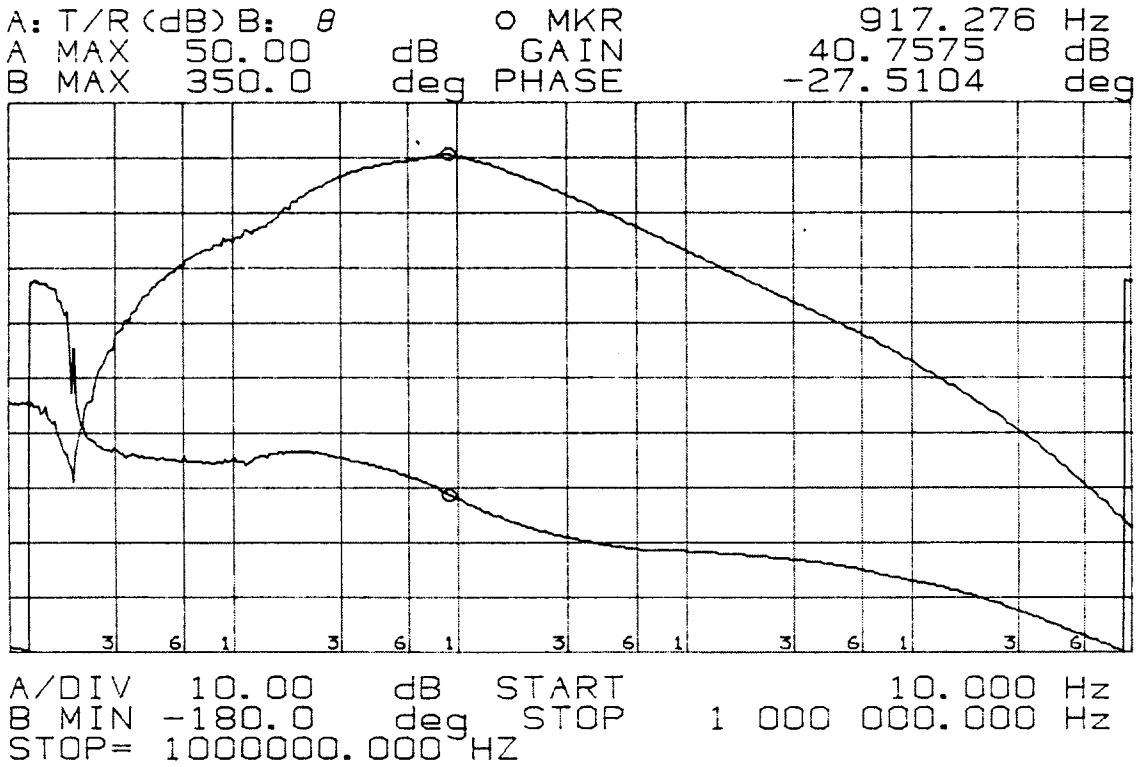

Fig. 15: The measured frequency response of an etched-out STIM-2B probe amplifier.

In summary, the active stimulating probe mask set STIM-2B/3B was completed and etched out. Testing of the etched-out probes demonstrated their complete functionality, both the digital and analog portions. The final etch-out was successful in that the circuit areas remained protected due to the use of dielectric bridge compensation. Tests of our microfuses has demonstrated their feasibility and usefulness. During the coming quarter, we plan to build up several 3D arrays using the STIM-3B probe design. We also plan to begin *in-vivo* testing of the STIM-2B probe design and move forward in the design of a high-end 3D stimulation array which will include on-chip current generation and have 512-1024 sites.

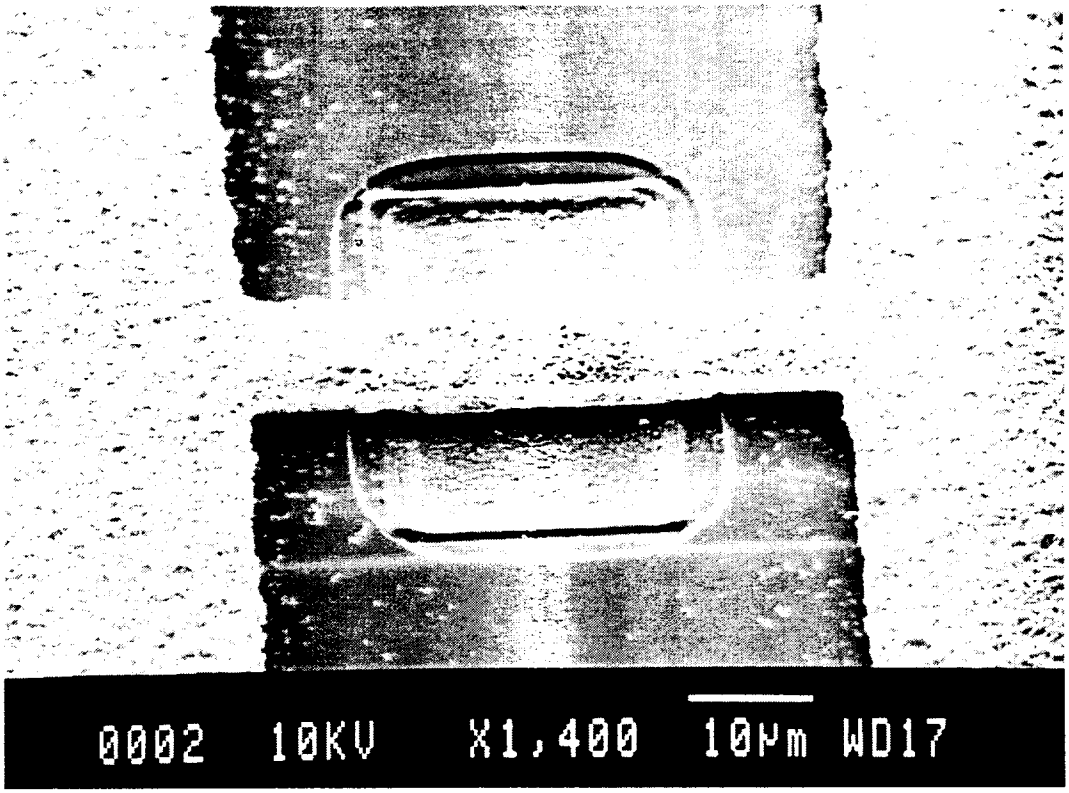

Fig. 16: A SEM photograph of a electroplated gold microfuse for use in programming 3D array platforms.

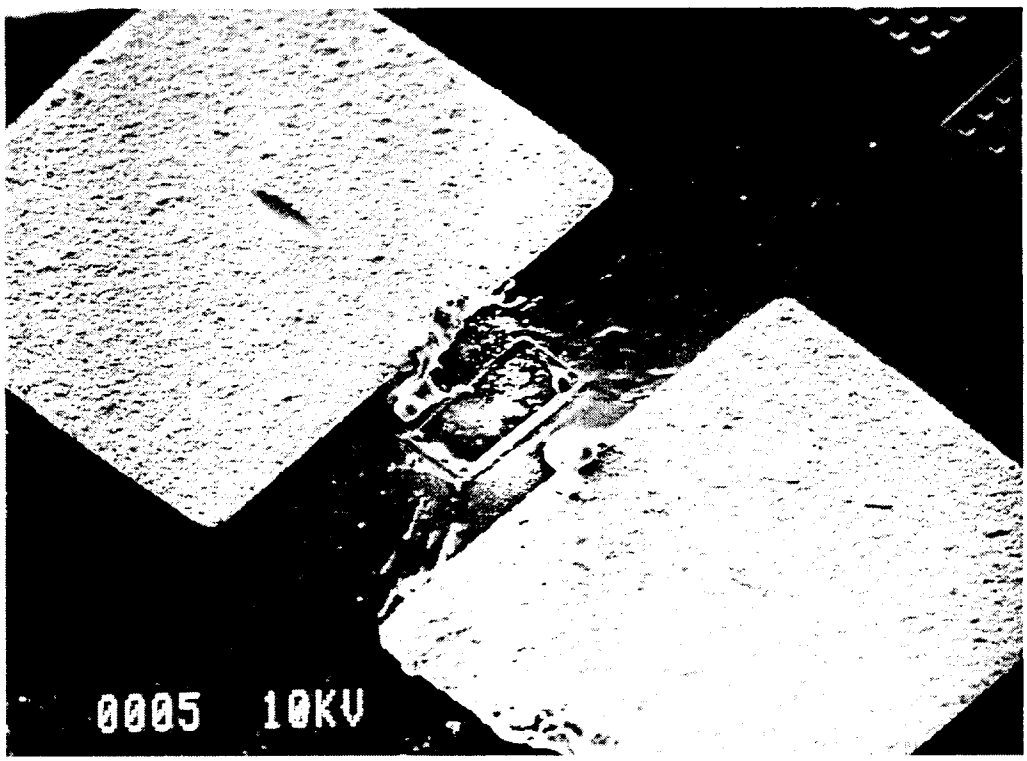

Fig. 17: A SEM photograph of a microfuse that has been blown by applying 2V.

4. *An External Interface to Micromachined Stimulating Probes*

We have designed and constructed a prototype interface system for active stimulating probes, as described in previous reports. This system currently exists as a functional wirewrap prototype but with limited maximum frequency of stimulation. The goal of the prototype was to allow for easy testing and modification of the system design. The realization of our design on a printed circuit board carrier (in progress) will enable the full functionality and speed of our system.

We have also developed the necessary support software to allow graphical interaction with our hardware prototype from a remote computer. This software provides a simple interface to pulsatile stimulation with varying phase widths, driving currents, and repetition rates. The probe communication rate is also configurable from full speed (determined by the frequency of an on-board oscillator, up to 10 Mbits/second) down to a division by 256. Finally, the special probe functions of power-on reset and current testing are supported.

The graphical software interface also includes a command-line interpreter in a separate window which allows for fine-grain control over the remote system. Whereas the graphical component of the interface is intended as an easy-to-use method of performing common functions, the command-line interpreter can be used to effect any other function not supported by the graphical interface.

During the past quarter, we had the opportunity to integrate and test our external interface system with a working STIM-2B probe. Our experiments validated the functionality of the external system and the probe interface protocol. We were able to successfully send data words to the probe using the STIM-2B communications protocol. The data words were correctly interpreted by the probe, as verified by observing changes in stimulating sites. In addition, we verified the functionality of the probe power-on reset circuitry in response to negative-voltage pulses on the clock line.

We also verified the current stimulation path by sending pulsatile waveforms to the probe on one of the external current lines. These waveforms were observed at the selected stimulating site on the probe. We were able to vary both the phase duration and current magnitude using our graphical interface and see these changes reflected in the observed waveform. We did, however, observe a slow edge rise time which limited the minimum pulse phase duration to approximately 1 millisecond. The pulse driver circuitry will need to be re-designed in order to generate faster rise times, and thereby allow shorter-duration pulses. This work is currently in progress.

In the next quarter we will focus on completing the printed circuit board realization of our hardware design. Apart from the pulse driver circuitry, this will require minimal changes to the design itself (to incorporate mechanical items such as connectors). We expect to have working boards by the end of this coming quarter.

5. *Conclusions*

This program seeks to develop a family of thin-film stimulaing arrays for use in neural prostheses. During the past quarter, work has gone forward in a number of areas. We have continued to explore alternative processing options for defining the silicon substrate which shapes these probes, especially the use of a porous silicon sacrificial layer. Such layers can be undercut from the front so that the probes do not have to be released by

etching completely through the wafer. Furthermore, they can be released at room temperature such that the etchants involved do not attack any of the other materials used. Previously, a boron-doped buried layer was used for the porous sacrificial layer; however, during the past term, we have found that an n+ buried layer works better, outdiffuses less, and can be released using a single electrochemical electropolishing etch at end of process so that no actual porous silicon is involved. We are using this technique on a set of probes that are currently in fabrication. This set includes a 32-site 46mm-long stimulating probe for use in the cochlea. This study will be completed during the coming term and contrasted with the usual boron-diffused etch-stop process.

During the past term, the active probes STIM-2B and -3B have been completed. STIM-2B is a 64-site 4-channel 16-shank probe that routes each of the input channels to one of 16 sites under the control of a serial input data stream. These probes have been tested and found fully functional. The yield of the probes was high, reflecting the improved methods for protecting the active circuit areas mentioned in the past report. The maximum data input rate on the probes in our present test setup is 4MHz, very close to the design value. The current pattern launched by the probe can thus be altered in about 4μsec. All of the operating modes of the probes are functional, including power-on reset (POR) for site activation and the high-impedance test mode for testing leakage on the overall structure. Any of the selected sites can be used for recording or stimulation. The on-chip recording amplifiers have a maximum gain at 1KHz of at least 40dB and a low-frequency rolloff below 100Hz. These devices have been used with the external electronic interface developed for the stimulating probes and have been found to operate well. Undercut gold fuses have also been demonstrated for use in coding future 3D platforms to allow different numbers of the STIM-3B probes to be used as desired. The STIM-3B probes are also fully functional and are built around STIM-2B with the addition of an on-chip x-address register and wings for mounting in the 3D assembly.

During the coming term, we will complete the study of alternative substrate definition techniques and will test the STIM-2B probes in-vivo. In addition, several 3D arrays of STIM-3B probes will be assembled. We will then move to a final iteration of our 64-site 8-channel 16-shank probe with on-chip current generation, STIM-2, and its 3D counterpart, STIM-3.